Structural Engineering and Mechanics, Vol. 44, No. 4 (2012) 465-485
DOI: http://dx.doi.org/10.12989/sem.2012.44.4.465

Analytical modelling of multilayer beams with compliant interfaces

L. Škec[1a], S. Schnabl*[2], I. Planinc[2b] and G. Jelenić[1b]

[1]*University of Rijeka, Faculty of Civil Engineering, Radmile Matejčić 3, 51000 Rijeka, Croatia*
[2]*University of Ljubljana, Faculty of Civil and Geodetic Engineering, Jamova 2, SI1115 Ljubljana, Slovenia*

(Received March 21, 2012, Revised October 22, 2012, Accepted October 24, 2012)

Abstract. Different mathematical models are proposed and their analytical solutions derived for the analysis of linear elastic Reissner's multilayer beams. The models take into account different combinations of contact plane conditions, different material properties of individual layers, different transverse shear deformations of each layer, and different boundary conditions of the layers. The analytical studies are carried out to evaluate the influence of different contact conditions on the static and kinematic quantities. A considerable difference of the results between the models is obtained.

Keywords: layered structures; delamination; analytical modelling; laminate mechanics; interlayer slip

1. Introduction

Composite structural elements are made of two or more components from one or more different materials in a single cross section. The basic idea is to combine the components in such a way that each of them fulfils the function for which its material characteristics are best suited. Due to this optimized performance of their components, the composite systems are economical and have a high bearing capacity. They are widely used in structures like steel-concrete composite beams, wood-steel concrete floors, coupled shear walls, sandwich beams, concrete beams externally reinforced with laminates and many more. The mechanical behaviour of these structures largely depends on the type of the connection between the layers. The use of mechanical shear connectors such as nails, screws and bolts is very common, but they provide only a partial interaction between the layers, thus the interlayer slip and uplift occur. Therefore, a partial interaction has to be taken into consideration in the mechanical analysis of multilayered structures. To this end, a large number of references exist on this very interesting topic. Among many others, a few examples are given here. Attard and Hunt (2008) presented a hyperelastic formulation of a sandwich column buckling where interlayer slip and uplift were neglected. Similar problems but with neglecting the effect of interlayer slip and uplift on mechanical behaviour of layered structures were proposed by Bareisis (2006) and Vu-Quoc *et al.* (1996). Taking into account the interlayer slip but neglecting the interlayer uplift was analyzed

*Corresponding author, Assistant Professor, E-mail: simon.schnabl@fgg.uni-lj.si
[a]Ph.D. Student
[b]Professor

by Frostig (2003), Girhammar and Pan (2007), Kryžanowski *et al*. (2009), Schnabl *et al*. (2006, 2007, 2010, 2011), Sousa and da Silva (2010), and McCutheon (1986).

Much less literature is available on mechanical analysis of multilayer beams where both interlayer slip and uplift were taken into account, see e.g. (Adekola 1968, Gara *et al.* 2006, Kroflič 2010a, b, 2011, Nquyen *et al.* 2001, Ranzi *et al.* 2006, 2010). Recently, Schnabl and Planinc (2012) applied both interlayer slip and uplift in the buckling analysis of two-layer composite columns where transverse shear deformation is also taken into consideration.

However, as far as the authors' knowledge is concerned it seems that there is no systematic analysis in the open literature for analytical modelling of bending of multilayer beams where different combinations of contact conditions are considered.

The aim of the present paper is to derive analytical models for bending of multilayer beams with various combinations of contact conditions. To this end, it is shown how to reformulate the governing equations in order to get well conditioned systems of generalized equations. In this paper, four characteristic analytical models are proposed.

2. Analytical model

2.1 Assumptions

A model of a planar multilayer beam composed of N layers and $N-1$ contact planes is studied with the following assumptions: (1) material is linear elastic; (2) displacements, rotations and strains are small; (3) shear strains are taken into account (the Timoshenko beam); (4) normal strains vary linearly over each layer (the Bernoulli hypothesis); (5) friction between the layers is neglected or is taken into account indirectly through the material models of the connection; (6) cross sections are symmetrical with respect to the plane of deformation and remain unchanged in the form and size during deformation; (7) both transverse and longitudinal separations between the layers are possible but they are assumed to be mutually independent; and (8) loading of a multilayer beam is symmetrical with regard to the plane of deformation.

2.2 Governing equations

An initially straight, planar, multilayer beam element of undeformed length L is considered, of which two adjacent layers i and $i+1$ separated by a contact plane α are shown in Fig. 1. The beam is placed in the (X, Z) plane of a spatial Cartesian coordinate system with coordinates (X, Y, Z) and unit base vectors $\mathbf{E}_X$, $\mathbf{E}_Y$, and $\mathbf{E}_Z$. Each layer has its own reference axis which coincides with the layer's centroidal axis. The reference axis of an arbitrary layer i is denoted as x^i in the undeformed configuration and $\bar{x}^i$ in the deformed configuration. The material particles of each layer are indentified by material coordinates $x^i, y^i, z^i (i = 1, \ldots, N)$. Besides, the material coordinate x^i of each layer is identical with its reference axis. In addition, it is assumed that $x^1 = x^2 = \ldots = x^N = x$. The multilayer beam element is subjected to the action of the distributed load $\mathbf{p}^i = p_X^i \boldsymbol{E}_X + p_Z^i \boldsymbol{E}_Z$ and the distributed moment $\mathbf{m}^i = m_Y^i \mathbf{E}_Y$ along the length of each layer. A differential segment of length dx of layer i with the applied loading with respect to the reference axis, the cross-sectional equilibrium forces and bending moments, and contact tractions in tangential and normal directions $p_{t,\alpha-1}$, $p_{t,\alpha}$, $p_{n,\alpha-1}$, and $p_{n,\alpha}$ is shown in Fig. 2.

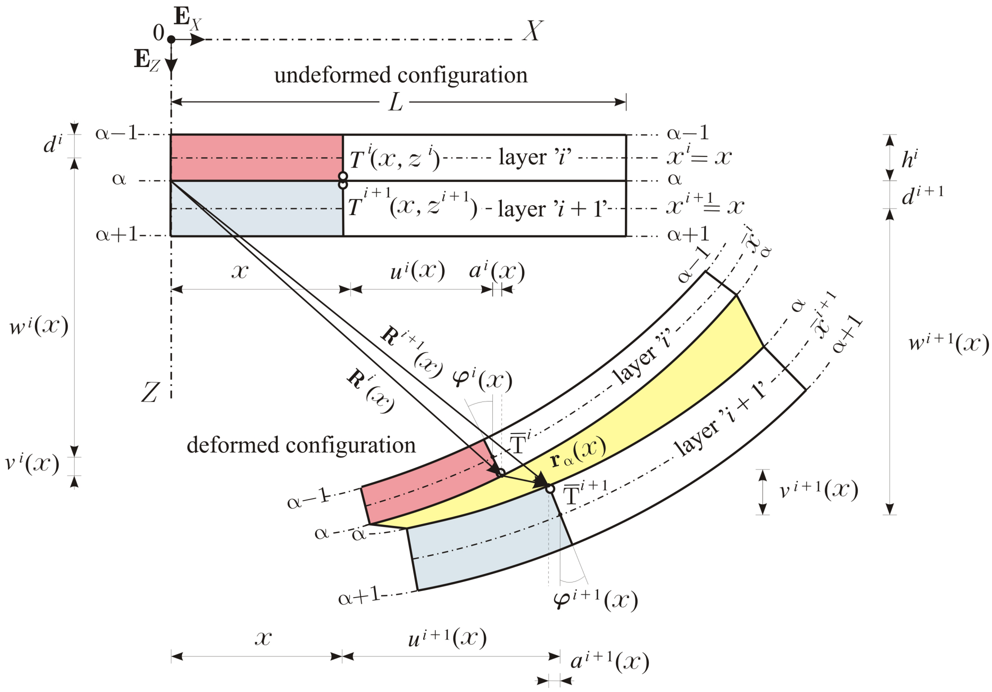

Fig. 1 Undeformed and deformed configuration of a multilayer beam

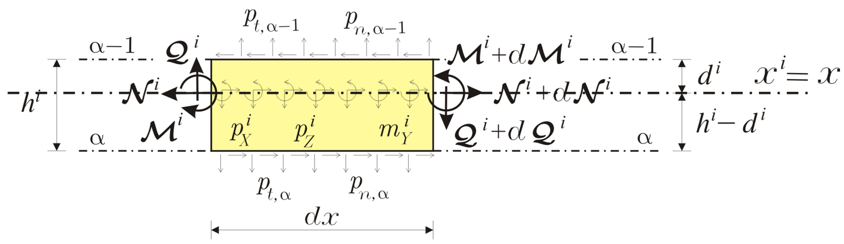

Fig. 2 Internal forces and interlayer tractions in a multilayer beam element

External point forces and moments can be applied only at the ends of the multilayer beam element and are introduced via boundary conditions. The system of linear governing equations of the multilayer beam is obtained using a consistent linearization of governing nonlinear equations of a Reissner planar beam in the undeformed initial configuration (Reissner 1972). Thus, the linearized system of governing equations consists of kinematic, equilibrium and constitutive equations with accompanying boundary conditions of each layer and the constraining equations that assemble each layer into a multilayer beam.

2.2.1 Kinematic equations

The kinematic equations listed below define the relationship between the displacements and strains for an arbitrary layer i (i = 1, 2,..., N)

$$
\begin{aligned}
u^{i\prime} - \varepsilon^i &= 0 \\
w^{i\prime} + \varphi^i - \gamma^i &= 0 \\
\varphi^{i\prime} - \kappa^i &= 0
\end{aligned} \tag{1}
$$

In Eq. (1), u^i, w^i, φ^i denote the components of the displacement and rotation vector of the ith layer at the reference axis $x^i = x$ with respect to the base vectors $\mathbf{E}_X$, $\mathbf{E}_Y$, and $\mathbf{E}_Z$, respectively. The prime $(\bullet)'$ denotes the derivative with respect to x. The extensional strain of the reference axis of the ith layer, the shear and the bending strain of the corresponding cross section of the ith layer are denoted by ε^i, γ^i and κ^i, respectively.

2.2.2 Equilibrium equations

The relationship between the loads applied on the layer i, the corresponding internal equilibrium forces and the distributed contact tractions are defined by the equilibrium equations derived from Fig. 2, (i = 1, 2,..., N)

$$
\begin{aligned}
\mathcal{N}^{i\prime} + p_X^i - p_{t,\alpha-1} + p_{t,\alpha} &= 0 \\
\mathcal{Q}^{i\prime} + p_Z^i - p_{n,\alpha-1} + p_{n,\alpha} &= 0 \\
\mathcal{M}^{i\prime} - \mathcal{Q}^i + m_Y^i + p_{t,\alpha-1} d^i + p_{t,\alpha}(h^i - d^i) &= 0
\end{aligned} \tag{2}
$$

where $\mathcal{N}^i$ and $\mathcal{Q}^i$ represent the axial and shear equilibrium forces while $\mathcal{M}^i$ is the equilibrium bending moment of the ith layer. On the other hand, p_X^i, p_Z^i, and m_Y^i are the distributed loads on ith layer given with respect to the reference axis $x^i = x$. The tangential and the normal interlayer contact tractions on the contact plane α are denoted by $p_{t,\alpha}$ and $p_{n,\alpha}$. On the outer planes of the multilayer beam no contact exists, thus

$$
\begin{aligned}
p_{t,\alpha 0} = p_{n,\alpha 0} &= 0 \\
p_{t,\alpha N} = p_{n,\alpha N} &= 0
\end{aligned} \tag{3}
$$

2.2.3 Constitutive equations

The constitutive internal forces $\mathcal{N}_C^i, \mathcal{Q}_C^i$, and $\mathcal{M}_C^i$ are related to the equilibrium internal forces $\mathcal{N}^i, \mathcal{Q}^i$, and $\mathcal{M}^i$ by the following constitutive equations (i = 1, 2,..., N)

$$
\begin{aligned}
\mathcal{N}^i - \mathcal{N}_C^i &= 0 \\
\mathcal{Q}^i - \mathcal{Q}_C^i &= 0 \\
\mathcal{M}^i - \mathcal{M}_C^i &= 0
\end{aligned} \tag{4}
$$

In the case of a linear elastic material and when the layer reference axis coincides with its centroidal axis, the constitutive forces are given by the linear relations with respect to ε^i, κ^i, and γ^i (Hjelmstad 2005), (i = 1, 2,..., N)

$$\mathcal{N}_C^i = E^i A^i \varepsilon^i = C_1^i \varepsilon^i$$
$$\mathcal{Q}_C^i = k_y^i G^i A^i \gamma^i = C_2^i \gamma^i$$
$$\mathcal{M}_C^i = E^i J^i \kappa^i = C_3^i \kappa^i \tag{5}$$

In Eqs. (5), E^i and G^i are the elastic and shear modulus, A^i denotes the area of the cross section, and J^i is the second moment of area of the ith layer with respect to the reference axis $x^i = x$. The shear coefficient of the cross section of the ith layer is denoted by k_y^i. For rectangular cross sections and isotropic material this coefficient is 5/6 (Cowper 1966).

2.2.4 Constraining equations

The constraining equations define the conditions by means of which an individual layer i is assembled into a multilayer beam. When a material point on the contact plane α between layers i and $i+1$ is observed (see Fig. 1), it can be identified in the undeformed configuration with points $T^i(x, z^i = h^i - d^i)$ and $T^{i+1}(x, z^{i+1} = -d^i)$, the first one on the lower edge of the upper layer i and the second one on the upper edge of the lower layer $i+1$. In the deformed configuration these two points become separated due to an interlayer separation. Vectors $\mathbf{R}^i(x, z^i = h^i - d^i)$ and $\mathbf{R}^{i+1}(x, z^{i+1} = -d^i)$ determine the position of points $\overline{T}^i$ and $\overline{T}^{i+1}$ in the deformed configuration

$$\mathbf{R}^i(x, z^i) = (x + u^i(x) + a^i(x, z^i))\mathbf{E}_X + (d^i - h^i + w^i(x) + v^i(x, z^i))\mathbf{E}_Z$$
$$\mathbf{R}^{i+1}(x, z^{i+1}) = (x + u^{i+1}(x) - a^{i+1}(x, z^{i+1}))\mathbf{E}_X + (d^{i+1} + w^{i+1}(x) - v^{i+1}(x, z^{i+1}))\mathbf{E}_Z \tag{6}$$

where $a^i(x, z^i) = (h^i - d^i)\sin\varphi^i(x)$, $a^{i+1}(x, z^{i+1}) = d^{i+1}\sin\varphi^{i+1}(x)$, $v^i(x, z^i) = (h^i - d^i)\cos\varphi^i(x)$ and $v^{i+1}(x, z^{i+1}) = d^{i+1}\cos\varphi^{i+1}(x)$. Corresponding to the assumption of small displacements and rotations, the vector of separation of points $\overline{T}^i$ and $\overline{T}^{i+1}$

$$\mathbf{r}_\alpha(x, z^i, z^{i+1}) = \mathbf{R}^{i+1}(x, z^{i+1}) - \mathbf{R}^i(x, z^i) \ \ (\alpha = 1, 2, \ldots, N-1 \text{ and } i = \alpha)\text{, reads}$$
$$\mathbf{r}_\alpha(x, z^i, z^{i+1}) = (u^{i+1}(x) - u^i(x) - d^{i+1}\varphi^{i+1}(x) - (h^i - d^i)\varphi^i(x))\mathbf{E}_X + (w^{i+1}(x) - w^i(x))\mathbf{E}_Z \tag{7}$$

An interlayer slip between the adjacent layers is denoted by Δu_α and can be defined from Eq. (7) as ($\alpha = 1, 2, \ldots, N-1$ and $i = \alpha$)

$$\Delta u_\alpha = u^{i+1} - u^i - d^{i+1}\varphi^{i+1} - (h^i - d^i)\varphi^i \tag{8}$$

Since all the quantities in Eq. (8) are functions of material coordinate x, the notation of the argument x is abandoned. The interlayer uplift (vertical separation) is marked by Δw_α and defined from Eq. (7) as ($\alpha = 1, 2, \ldots, N-1$ and $i = \alpha$)

$$\Delta w_\alpha = w^{i+1} - w^i \tag{9}$$

The term interlayer distortion, $\Delta\varphi_\alpha$, is introduced as well to describe the difference between the rotation angles of adjacent layers as ($\alpha = 1, 2, \ldots, N-1$ and $i = \alpha$)

$$\Delta\varphi_\alpha = \varphi^{i+1} - \varphi^i \tag{10}$$

In general, flexibility of the contact highly depends on the way the contact is enforced. A constitutive law of the connection between the layers generally assumes a nonlinear relationship between contact displacements and interlayer tractions (Alfano and Crisfield 2001, Volokh and Needleman 2002). In the present paper, as generally proposed in the structural engineering practice, a linear constitutive law of the incomplete connection between the layers is assumed, see e.g. (Adekola 1968, Kroflič *et al.* 2010a, Schnabl *et al.* 2007). For the contact plane α, a linear uncoupled constitutive law of the connection between the layers can be written as ($\alpha = 1, 2,..., N-1$)

$$\begin{aligned} p_{t,\alpha} &= K_{t,\alpha}\Delta u_\alpha \\ p_{n,\alpha} &= K_{n,\alpha}\Delta w_\alpha \end{aligned} \tag{11}$$

where $K_{t,\alpha}$ and $K_{n,\alpha}$ are the slip and uplift moduli at the interlayer surface. On the other hand, the rotational degree of freedom in the contact defined e.g., as

$$m_{Y,\alpha} = K_{\varphi,\alpha}\Delta\varphi_\alpha \tag{12}$$

is in this paper not taken into account. With Eq. (10) only the difference of the cross sectional rotations are defined which is due to different transverse shear deformations of the layers. Eq. (11) can be used only in case when interlayer displacements are realized, thus $\Delta u_\alpha \neq 0$ and/or $\Delta w_\alpha \neq 0$. For example, in the case when $\Delta u_\alpha = 0$ from Eq. (11) it follows that $p_{t,\alpha} = 0$. That is obviously incorrect, since interlayer tractions also appear when interlayer displacements are absent. This former contradiction originates from the fact that in the limiting case, i.e., $K_{t,\alpha} \to \infty$ and $K_{n,\alpha} \to \infty$, the system of governing equations of a multilayer composite beam becomes singular (Hozjan *et al.* 2012). In these cases, the governing equations should be reformulated in a way that will be described below. Note that when $\Delta u_\alpha = 0$, the tangential contact tractions $p_{t,\alpha}$ are calculated from the equilibrium equations, i.e. Eq. (2). Similarly, when $\Delta w_\alpha = 0$, the same equilibrium equations are used to express $p_{n,\alpha}$, as well.

2.3 Basic models

The interlayer degrees of freedom can be described using Δu_α, Δw_α, and $\Delta\varphi_\alpha$ $(\alpha = 1,2,\ldots,N-1)$. By allowing or constraining a specific degree of freedom in the contact plane, $2^3(N-1)$ different combinations of contact plane conditions are introduced. In the present paper only four basic and most common models of different connections between the layers are elaborated although models where the constraining equations are different for each contact plane can be formulated in a similar manner. These common models and their corresponding interlayer degrees of freedom are presented in Table 1. The model M_{000} obviously reintroduces the Bernoulli hypothesis over the entire cross-section (thus enabling the problems in which $K_{t,\alpha} \to \infty, K_{n,\alpha} \to \infty$ and $K_{\varphi,\alpha} \to \infty$ to be accurately simulated), while the M_{001} relaxes this hypothesis to make it hold for each layer separately. Therefore, the problems in which $K_{t,\alpha} \to \infty$ and $K_{n,\alpha} \to \infty$, but $K_{\varphi,\alpha}$ remains finite may be accurately simulated using this model. In the models M_{101} and M_{111} the deformed cross-sections are not requested to remain continuous. Additionally, the model M_{101} obviously serves to simulate accurately the situations in which $K_{n,\alpha} \to \infty$.

Table 1 Basic models with corresponding interlayer degrees of freedom

MODEL	Δu	Δw	$\Delta\varphi$
M_{000}	×	×	×
M_{001}	×	×	√
M_{101}	√	×	√
M_{111}	√	√	√

×: zero value; √: non-zero value.

2.3.1 Model M_{000} - the standard beam model

The contact plane conditions for the model M_{000} according to Table 1 are described by the following expressions ($i = 1, 2, \ldots, N-1$)

$$
\begin{aligned}
u^{i+1} &= u^i + (h^i - d^i + d^{i+1})\varphi^i \\
w^i &= w^{i+1} = w^k \\
\varphi^i &= \varphi^{i+1} = \varphi^k \\
\varepsilon^{i+1} &= \varepsilon^i + (h^i - d^i + d^{i+1})\kappa^i \\
\gamma^i &= \gamma^{i+1} = \gamma^k \\
\kappa^i &= \kappa^{i+1} = \kappa^k
\end{aligned} \tag{13}
$$

where the index k marks an arbitrary layer from $i = 1, \ldots, N$. After considering relations (13) in the general governing equations of the multilayer beam (1)-(5), the basic equations of the model M_{000} are the following

$$u^{k\prime} - \varepsilon^k = 0, \quad \mathcal{N}' + \sum_{i=1}^{N} p_X^i = 0$$

$$w^{k\prime} + \varphi^k - \gamma^k = 0, \quad \mathcal{Q}' + \sum_{i=1}^{N} p_Z^i = 0$$

$$\varphi^{k\prime} - \kappa^k = 0, \quad \mathcal{M}' - \mathcal{Q} + \sum_{i=1}^{N} m_Y^i + \sum_{i=1}^{N} (p_{t,i-1} d^i + p_{t,i}(h^i - d^i)) = 0 \text{ or}$$

$$\mathcal{M}'_{TOT} - \mathcal{Q} + \sum_{i=1}^{N} m_Y^i = 0$$

$$\mathcal{N} = \sum_{i=1}^{N} C_1^i \varepsilon^i, \quad \mathcal{Q} = \sum_{i=1}^{N} C_2^i \gamma^i, \quad \mathcal{M} = \sum_{i=1}^{N} C_3^i \kappa^i \tag{14}$$

where

$$\mathcal{N} = \sum_i^N \mathcal{N}^i, \quad \mathcal{Q} = \sum_i^N \mathcal{Q}^i, \quad \mathcal{M} = \sum_i^N \mathcal{M}^i$$

Since every layer has its own separate reference axis, $\mathcal{M}$ is not the total cross-sectional bending moment of a composite beam because the axial forces $\mathcal{N}^i$, that are mutually dislocated, contribute to the total bending moment as well. Thus, $\mathcal{M}_{TOT} = \mathcal{M} + \sum_i^N \mathcal{N}^i r^i$, where r^i is the distance between the reference axis of the ith layer and the arbitrary axis with respect to which the total bending moment is computed. The system (14) is a system of nine equations for nine unknown functions u^k, w^k, φ^k, $\mathcal{N}$, $\mathcal{Q}$, $\mathcal{M}$ or $\mathcal{M}_{TOT}$, ε^k, γ^k, and κ^k where the additional functions $p_{t,i}$ are expressed in terms of strains ε^k and γ^k using (2), (4) and (5). Using the last three equations of system (13), we express ε^k, γ^k and κ^k in the system (14) in terms of u^k, w^k and φ^k, finally obtaining a system of six ordinary linear differential equations with constant coefficients for six unknown functions u^k, w^k, φ^k, $\mathcal{N}$, $\mathcal{Q}$, and $\mathcal{M}$ or $\mathcal{M}_{TOT}$. This reduced system can be solved analytically with the following boundary conditions from which six constants of integration are found

$$\begin{aligned}
f_1^0 \mathcal{N}(0) + (1-f_1^0) u^k(0) &= f_1^0 S_1^0 + (1-f_1^0) U_1^k(0) \\
f_2^0 \mathcal{Q}(0) + (1-f_2^0) w^k(0) &= f_2^0 S_2^0 + (1-f_2^0) U_2^k(0) \\
f_3^0 \mathcal{M}(0) + (1-f_3^0) \varphi^k(0) &= f_3^0 S_3^0 + (1-f_3^0) U_3^k(0) \\
f_1^L \mathcal{N}(L) + (1-f_1^L) u^k(L) &= f_1^L S_1^L + (1-f_1^L) U_1^k(L) \\
f_2^L \mathcal{Q}(L) + (1-f_2^L) w^k(L) &= f_2^L S_2^L + (1-f_2^L) U_2^k(L) \\
f_3^L \mathcal{M}(L) + (1-f_3^L) \varphi^k(L) &= f_3^L S_3^L + (1-f_3^L) U_3^k(L)
\end{aligned} \tag{15}$$

where $S_n^0 = \sum_{i=1}^N S_n^{0,i}$ and $S_n^L = \sum_{i=1}^N S_n^{L,i}$ (n = 1, 2, 3), are the external end point forces and moments of the beam, while U_n^0 and U_n^L are the displacements and the rotations at the beam ends that are identical for all layers. The coefficients f_n^0 and f_n^L have values 1 or 0 depending on the type of the support at the beam ends.

2.3.2 Model M_{001}

This model is defined by the contact plane conditions described below $(i = 1, 2, \ldots, N-1)$

$$\begin{aligned}
u^{i+1} &= u^i + d^{i+1}\varphi^{i+1} + (h^i - d^i)\varphi^i \\
w^i &= w^{i+1} = w^k \\
\varepsilon^{i+1} &= \varepsilon^i + d^{i+1}\kappa^{i+1} + (h^i - d^i)\kappa^i \\
\gamma^{i+1} &= \gamma^i + \varphi^{i+1} - \varphi^i
\end{aligned} \tag{16}$$

The basic equations of the model are written by considering relations (16) as (i = 1, ..., N)

$$u^{k\prime} - \varepsilon^k = 0, \quad \mathcal{N}' + \sum_{i=1}^N p_X^i = 0$$

$$w^{k\prime} + \varphi^k - \gamma^k = 0\,, \quad \mathcal{Q}' + \sum_{i=1}^{N} p_Z^i = 0$$

$$\varphi^{i\prime} - \kappa^i = 0\,, \quad \mathcal{M}^{i\prime} - \mathcal{Q}^i + m_Y^i + p_{t,\,i-1}d^i + p_{t,\,i}(h^i - d^i) = 0$$

$$\mathcal{N} = \sum_{i=1}^{N} C_1^i \varepsilon^i\,, \quad \mathcal{Q} = \sum_{i=1}^{N} C_2^i \gamma^i\,, \quad \mathcal{M}^i = C_3^i \kappa^i \tag{17}$$

Similarly as in the model M_{000}, the contact tractions $p_{t,\,\alpha}$ $(\alpha = 1, 2, \ldots, N-1)$ are expressed via the strains ε^k, γ^k, and κ^i which are further expressed via displacements u^k, w^k, and φ^k, (i = 1, 2, ..., N). This allows reducing the system (17) to a system of $4 + 2N$ linear first-order ordinary differential equations with constants coefficients for the same number of unknown functions: $u^k, w^k, \mathcal{N}, \mathcal{Q}, \varphi^i$, and $\mathcal{M}^i$ (i = 1, 2, ..., N). These functions are determined after the system is solved in conjunction with the following boundary conditions (i = 1, 2,..., N)

$$\begin{aligned}
f_1^0 \mathcal{N}(0) + (1 - f_1^0) u^k(0) &= f_1^0 S_1^0 + (1 - f_1^0) U_1^0 \\
f_2^0 \mathcal{Q}(0) + (1 - f_2^0) w^k(0) &= f_2^0 S_2^0 + (1 - f_2^0) U_2^0 \\
f_3^{0,\,i} \mathcal{M}^i(0) + (1 - f_3^{0,\,i}) \varphi^i(0) &= f_1^{0,\,i} S_3^{0,\,i} + (1 - f_3^{0,\,i}) U_3^{0,\,i} \\
f_1^L \mathcal{N}(L) + (1 - f_1^L) u^k(L) &= f_1^L S_1^L + (1 - f_1^L) U_1^L \\
f_2^L \mathcal{Q}(L) + (1 - f_2^L) w^k(L) &= f_2^L S_2^L + (1 - f_2^L) U_2^L \\
f_3^{L,\,i} \mathcal{M}^i(L) + (1 - f_3^{L,\,i}) \varphi^i(L) &= f_3^{L,\,i} S_3^{L,\,i} + (1 - f_3^{L,\,i}) U_3^{L,\,i}
\end{aligned} \tag{18}$$

where $S_n^0 = \Sigma_{i=1}^{N} S_n^{0,\,i}$ and $S_n^L = \Sigma_{i=1}^{N} S_n^{L,\,i}$ (n = 1, 2) and $f_3^{0,\,i}$ and $f_3^{L,\,i}$ are the boundary conditions coefficients at the beam ends for each layer i (i = 1, 2, ..., N). They have values 1 or 0 depending on the type of the support at the both ends of each layer. External moments and rotations at the ends of each layer are denoted by $S_3^{0,\,i}, S_3^{L,\,i}$ and $U_3^{0,\,i}, U_3^{L,\,i}$ respectively. In addition, note that U_1^0, U_2^0, U_1^L, and U_2^L are the same for all layers.

2.3.3 Model M_{101}

Using the contact conditions from Table 1, the following relations are derived ($\alpha = 1, 2, \ldots, N-1$ and $i = \alpha$)

$$\begin{aligned}
w^i &= w^{i+1} = w^k \\
\gamma^{i+1} &= \gamma^i + \varphi^{i+1} - \varphi^i \\
p_{t,\,\alpha} &= K_{t,\,\alpha} \Delta u_\alpha
\end{aligned} \tag{19}$$

The basic equations for the model M_{101} are presented below (i = 1, 2, ..., N)

$$u^{i\prime} - \varepsilon^i = 0\,, \quad \mathcal{N}^{i\prime} + p_X^i - p_{t,\,i-1} + p_{t,\,i} = 0$$

$$w^{k\prime} + \varphi^k - \gamma^k = 0\,, \quad \mathcal{Q}' + \sum_{i=1}^{N} p_Z^i = 0$$

$$\varphi^{i\prime} - \kappa^i = 0\,, \quad \mathcal{M}^{i\prime} - \mathcal{Q}^i + m_Y^i + p_{t,i}d^i + p_{t,i-1}(h^i - d^i) = 0$$
$$\mathcal{N}^i = C_1^i\varepsilon^i\,, \quad \mathcal{Q} = \sum_{i=1}^{N} C_2^i\gamma^i\,, \quad \mathcal{M}^i = C_3^i\kappa^i \tag{20}$$

The strains ε^i, γ^k and κ^i are expressed via internal forces $\mathcal{N}^i$, $\mathcal{Q}$ and $\mathcal{M}^i$ from the constitutive equations (last $2N + 1$ equations of the system (20)). The contact tractions $p_{t,\alpha}$ are expressed via displacements u^i and rotations φ^i from Eqs. (19) and (8). The system (20) is reduced to a system of $2 + 4N$ linear first-order ordinary differential equations with constant coefficients for the same number of unknown functions: $u^i, w^k, \varphi^i, \mathcal{N}^i, \mathcal{Q}$, and $\mathcal{M}^i$ (i = 1, 2,..., N). To solve this system the corresponding boundary conditions are considered

$$f_1^{0,i}\mathcal{N}^i(0) + (1 - f_1^{0,i})u^i(0) = f_1^{0,i}S_1^{0,i} + (1 - f_1^{0,i})U_1^{0,i}$$
$$f_2^0\mathcal{Q}(0) + (1 - f_2^0)w^k(0) = f_2^0 S_2^0 + (1 - f_2^0)U_2^0$$
$$f_3^{0,i}\mathcal{M}^i(0) + (1 - f_3^{0,i})\varphi^i(0) = f_3^{0,i}S_3^{0,i} + (1 - f_3^{0,i})U_3^{0,i}$$
$$f_1^{L,i}\mathcal{N}^i(L) + (1 - f_1^{L,i})u^i(L) = f_1^{L,i}S_1^{L,i} + (1 - f_1^{L,i})U_1^{L,i}$$
$$f_2^L\mathcal{Q}(L) + (1 - f_2^L)w^k(L) = f_2^L S_2^L + (1 - f_2^L)U_2^L$$
$$f_3^{L,i}\mathcal{M}^i(L) + (1 - f_3^{L,i})\varphi^i(L) = f_3^{L,i}S_3^{L,i} + (1 - f_3^{L,i})U_3^{L,i} \tag{21}$$

where $S_2^0 = \Sigma_{i=1}^N S_2^{0,i}$ and $S_2^L = \Sigma_{i=1}^N S_2^{L,i}$ while $f_1^{0,i}$ and $f_1^{L,i}$ $(i = 1, 2, \ldots, N)$ are the boundary conditions coefficients with values 0 or 1 depending on the type of support the ends of each layer. The external longitudinal point forces and horizontal displacements at the ends of each layer are denoted as $S_1^{0,i}, S_1^{L,i}$ a nd $U_1^{0,i}, U_1^{L,i}$ $(i = 1, 2, \ldots, N)$, respectively. Again, note that U_2^0 and U_2^L are the same for all layers.

2.3.4 Model M_{111}

The contact plane conditions for this model are expressed using only the constraining equations (11). The basic equations of this model are presented below $(i = 1, 2, \ldots, N)$

$$u^{i\prime} - \varepsilon^i = 0\,, \quad \mathcal{N}^{i\prime} + p_X^i - p_{t,i-1} + p_{t,i} = 0$$
$$w^{i\prime} + \varphi^i - \gamma^i = 0\,, \quad \mathcal{Q}^{i\prime} + p_Z^i - p_{n,i-1} + p_{n,i} = 0$$
$$\varphi^{i\prime} - \kappa^i = 0\,, \quad \mathcal{M}^{i\prime} - \mathcal{Q}^i + m_Y^i + p_{t,i-1}d^i + p_{t,i}(h^i - d^i) = 0$$
$$\mathcal{N}^i = C_1^i\varepsilon^i\,, \quad \mathcal{Q}^i = C_2^i\gamma^i\,, \quad \mathcal{M}^i = C_3^i\kappa^i \tag{22}$$

The strains ε^i, γ^i, and κ^i are expressed via internal forces $\mathcal{N}^i$, $\mathcal{Q}^i$, and $\mathcal{M}^i$ from the constitutive equations (last $3N$ equations in the system (22)) and the contact tractions $p_{t,\alpha}$ and $p_{n,\alpha}$ from Eq. (11). System (22) is reduced to a system of $6N$ linear first-order ordinary differential equations with constant coefficients for the same number of unknown functions: $u^i, w^i, \varphi^i, \mathcal{N}^i, \mathcal{Q}^i$, and $\mathcal{M}^i$ $(i = 1, 2, \ldots, N)$.

The corresponding boundary conditions are $(i = 1, 2, \ldots, N)$

$$
\begin{aligned}
f_1^{0,i}\mathcal{N}^i(0) + (1-f_1^{0,i})u^i(0) &= f_1^{0,i}S_1^{0,i} + (1-f_1^{0,i})U_1^{0,i} \\
f_2^{0,i}\mathcal{Q}^i(0) + (1-f_2^{0,i})w^i(0) &= f_2^{0,i}S_2^{0,i} + (1-f_2^{0,i})U_2^{0,i} \\
f_3^{0,i}\mathcal{M}^i(0) + (1-f_3^{0,i})\varphi^i(0) &= f_3^{0,i}S_3^{0,i} + (1-f_3^{0,i})U_3^{0,i} \\
f_1^{L,i}\mathcal{N}^i(L) + (1-f_1^{L,i})u^i(L) &= f_1^{L,i}S_1^{L,i} + (1-f_1^{L,i})U_1^{L,i} \\
f_2^{L,i}\mathcal{Q}^i(L) + (1-f_2^{L,i})w^i(L) &= f_2^{L,i}S_2^{L,i} + (1-f_2^{L,i})U_2^{L,i} \\
f_3^{L,i}\mathcal{M}^i(L) + (1-f_3^{L,i})\varphi^i(L) &= f_3^{L,i}S_3^{L,i} + (1-f_3^{L,i})U_3^{L,i}
\end{aligned} \tag{23}
$$

where $f_n^{0,i}$ and $f_n^{L,i}$ ($i = 1, 2, \ldots, N$ and n = 1, 2, 3) are the boundary conditions coefficients for each layer, while $S_n^{0,i}, S_n^{L,i}$ and $U_n^{0,i}, U_n^{L,i}$ ($i = 1, 2, \ldots, N$ and n = 1, 2, 3) are the external transverse point forces and vertical displacements at the ends of each layer, respectively.

3. Analytical solution

The reduced systems of generalized equilibrium Eqs. (14), (17), (20), and (22) are the systems of linear first-order ordinary differential equations with constant coefficients. Similarly, the systems of generalized equations of other mathematical models not introduced in the paper are also systems of linear first-order ordinary differential equations with constant coefficients. In general, such systems of equations can be written in the following compact form as

$$\mathbf{Y}'(x) = \mathbf{B}\mathbf{Y}(x) + \mathbf{g}, \quad \mathbf{Y}(0) = \mathbf{Y}_0 \tag{24}$$

where $\mathbf{Y}$ is the vector of unknown functions, $\mathbf{g}$ is the vector of external loading, $\mathbf{B}$ is the matrix of constant coefficients, and $\mathbf{Y}_0$ is the vector of boundary parameters that are determined from the boundary conditions of the multilayer beam. The solution of the inhomogeneous system of differential Eq. (24) is composed of homogeneous and particular solutions (Perko 2001)

$$\mathbf{Y}(x) = \exp(\mathbf{B}x)\left[\mathbf{Y}_0 + \int_0^x \exp(-\mathbf{B}\xi)\mathbf{g}\,d\xi\right] \tag{25}$$

When a multilayer beam is subjected only to point forces and moments, i.e., $\mathbf{g}$ = 0, the solution of (24) is composed of a homogeneous solution only

$$\mathbf{Y}(x) = \exp(\mathbf{B}x)\mathbf{Y}_0 \tag{26}$$

Similarly as in the case of homogeneous structures, the multilayer structures are composed of multilayer beams. In such cases, the analytical solution is obtained from the analytical solution of individual multilayer beam. The procedure is very similar to the finite element method.

4. Numerical results and discussion

Two numerical examples are analysed in detail in order to illustrate the present theory. In the first

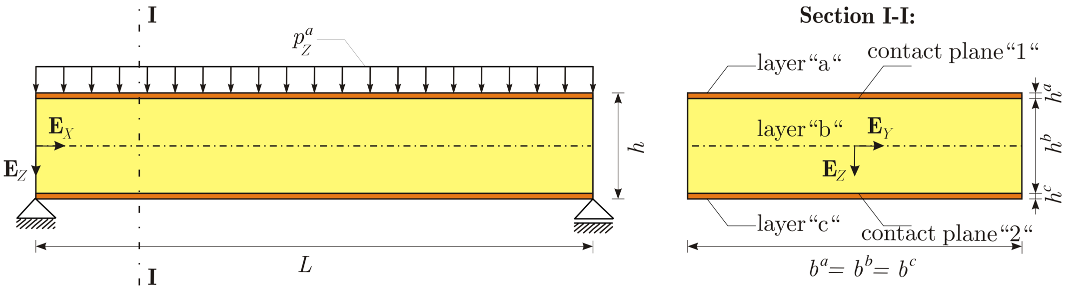

Fig. 3 Simply supported sandwich beam with uniformly distributed vertical load

example the influence of various parameters on the midspan vertical displacement of a sandwich beam has been investigated. The influence of contact discontinuity between the layers of a composite beam on its bearing capacity has been illustrated in the second example.

4.1 Simply supported sandwich beam with uniformly distributed load

A parametric study for this example has been performed on a simply supported sandwich beam subjected to a uniformly distributed load (see Fig. 3). The sandwich beam layers are denoted by $i = a, b, c$ and the contact planes by $\alpha = 1, 2$, respectively. The geometrical and material characteristics are the following: $L^i = L = 100$ mm, $h^a = h^c = 1$ mm, $h^b = 18$ mm, $b^i = 60$ mm, $E^a = E^c = 2 \cdot 10^4$ N/mm^2, $E^b = E^a/50$, $G^a = E^a/8$, $G^b = 3/4E^b$, $G^c = E^c/8$, $k_y^i = 5/6$. The uniformly distributed load, $p_Z^a = 2$ N/mm, is applied on the layer a.

Note that the values of the shear moduli fall outside the range of possible values for an isotropic material, but are perfectly acceptable e.g., for timber (Schnabl *et al.* 2007). Due to symmetry, only one half of the sandwich beam has been analysed, so that the boundary conditions are given as

$$\mathcal{N}^i(0) = \mathcal{N}^b(0) = 0, \; w^i(0) = 0, \; \mathcal{M}^i(0) = 0 \tag{27}$$

on the left-hand side of the beam, and

$$u^i(L/2) = 0, \; \mathcal{Q}^i(L/2) = 0, \; \varphi^i(L/2) = 0 \tag{28}$$

on the middle of the beam, where $i = a, b, c$. Defining the boundary conditions in this manner allows us to solve the problem where $K_{t,\alpha} = 0$, $(\alpha = 1, 2)$. In Table 2 the vertical displacements of the centroid axis at the midspan of the sandwich beam for different multilayer beam models are presented depending on the L/h ratio. For $L/h = 5$ the same characteristics as given above have been used, while for other L/h ratios only the length of the beam has been modified accordingly. A vertical displacement of a homogeneous beam according to the classical engineering theory proposed by Timoshenko (1940), $w_\infty = 5p_Z^aL^4/384EI_\infty + p_Z^aL^2/8k_yGA_\infty$, has been used as a reference vertical displacement, where $EI_\infty = EI_0 + E^aA^a((h^a+h^b)^2/4) + E^cA^c((h^b+h^c)^2/4)$, $EI_0 = \sum_{i=a}^{c} E^iI^i$ and $k_yGA_\infty = \sum_{i=a}^{c} k_y^iG_iA_i$. The non-dimensional vertical displacement, $\overline{w}_M = w_M/w_\infty$, is introduced, where w_M is the vertical displacements at the midspan of a sandwich beam for an arbitrary model M. Four values of the slip modulus $K_{t,\alpha}$ for $\alpha = 1, 2$ are analysed: 0, 1, 10 and 100 N/mm^2. The model M_{000} shows exactly the same behaviour as the homogeneous beam, which is due to its rigid interlayer connection ($\Delta u_\alpha = \Delta w_\alpha = \Delta\varphi_\alpha = 0$ where $\alpha = 1, 2$). The differences between the results of the models M_{000} and M_{001} range between approximately 7% for a moderately thick beam (L/h = 10) to more than about 53% for a very thick beam (L/h = 2). By allowing the interlayer slip to occur, the vertical displacements at the midspan increase more considerably, especially as interaction between the layers gets weaker ($K_{t,\alpha} \to 0$). In the last column in Table 2 the non-dimensional vertical displacement for a sandwich beam with no interaction between the layers is given according to the Bernoulli beam theory as $\overline{w}_0 = w_0/w_\infty$ with $w_0 = 5p_A^a L^4 / 384EI_0$. As expected, the results of the model M_{101} with $K_{t,\alpha} = 0$ approach this solution as the beam becomes thinner.

The core thickness ratio influence is described by h^b/h, where h^b is the core's height while h is the total height of the sandwich beam cross-section. By changing the core height but keeping the total height constant (h = 20 mm) the vertical displacement at the midspan is studied (see Fig. 4). The values of $K_{t,\alpha}$ are written in the parentheses next to M_{101} in the legend to Fig. 4. It is noticed that w increases monotonically with h^b/h ratio for the models M_{000} and M_{001}, but for the model M_{101} an extreme value of w appears for the presented values of $K_{t,\alpha}$. For $K_{t,\alpha} = 0$, the maximum vertical displacement at the midspan is obtained for $h^c/h \approx 0.8$, while for the higher stiffnesses $K_{t,\alpha}$ the maximum vertical displacement occurs at lower h_b/h ratios. From the expression for w_0, it can be easily shown that the beam stiffness EI_0 has a maximum at $h^b/h = 0.7795$ which coincides very well with the present result for the model M_{101} with $K_{t,\alpha} = 0$.

Table 2 Non-dimensional vertical displacement ($\overline{w}_M = w_M/w_\infty$) at the midspan for various contact plane conditions depending on L/h ratio

L/h	w_∞ (mm)	M_{000}	M_{001}	M_{101}				$\overline{w}_0$
				$K_{t,\alpha^\star} = 100^*$	$K_{t,\alpha^\star} = 10^*$	$K_{t,\alpha^\star} = 1^*$	$K_{t,\alpha^\star} = 0^*$	
2	0.00106	1.00000	1.53262	5.58215	6.51117	6.62796	6.64128	5.29600
5	0.01621	1.00000	1.21944	6.09954	12.28912	13.88957	14.09633	13.54423
7	0.05321	1.00000	1.13108	4.69571	12.52822	15.71016	16.17645	15.84678
10	0.20161	1.00000	1.07063	3.24534	11.06386	16.58495	17.59765	17.42006

$^\star\alpha = a, b$; * in N/mm^2

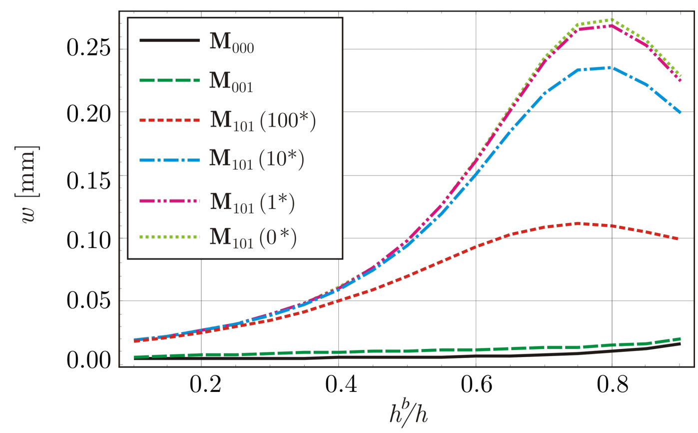

Fig. 4 w versus h_b/h for different contact plane conditions. * means $K_{t,\alpha}$ in N/mm^2

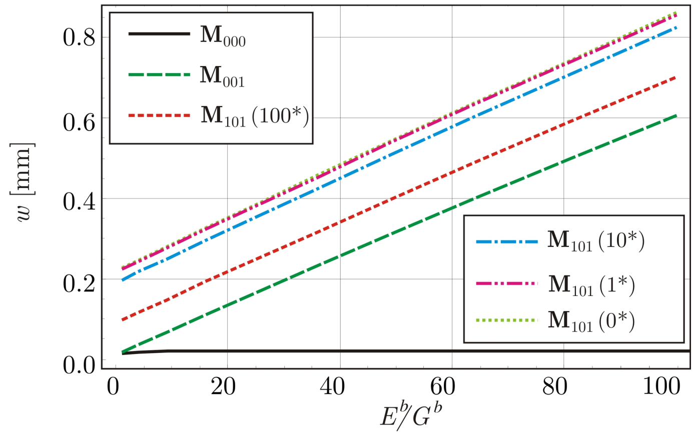

Fig. 5 w versus E^b/G^b for different contact plane conditions. * means $K_{t,\alpha}$ in N/mm^2

The influence of the core elastic-to-shear modulus ratio, E^b/G^b, on midspan vertical displacements is displayed in Fig. 5. The range $0 < E^b/G^b < 100$ is reasonable only for anisotropic materials. A considerable difference of the results between the models M_{000} and M_{001} is observed by the interlayer distortion which is dependent on the layer's shear modulus. In case when $\Delta w_\alpha = 0$ it follows that $\Delta\varphi_\alpha = \gamma^{i+1} - \gamma^i = \mathcal{Q}^{i+1}/C_2^{i+1} - \mathcal{Q}^i/C_2^i$ (see Eq. (5)), which means that the higher values of the shear moduli produce smaller values of the interlayer distortion and thus smaller vertical displacements. Obviously, as the E^b/G^b ratio increases the differences between the models M_{000} and M_{001} become more pronounced. For models M_{101} the interlayer slip (depending on different $K_{t,\alpha}$ values) causes a considerable increase in the vertical displacements in comparison to model M_{001}. It is noticed that all models have almost linear $E_b/G_b - w$ relationship.

4.2 Contact discontinuity influence studies

A simply supported two-layer beam is analysed in this example (see Fig. 6). Layers are marked by $i = a, b$. The geometrical and material characteristics are as follows: $L^i = L = 200$ cm, $h^i = 10$ cm, $b^i = 20$ cm, $E^i = 800$ kN/cm^2, $G^i = E^i/16$, $k_y^i = 5/6$. The uniformly distributed load, $p_Z^b = 0.2$ kN/cm, is applied at the reference layer of the lower layer b. The beam is divided into three segments, namely e_1, e_2 and e_3, whose lengths are L_1, L_2, and L_3, respectively. The central segment is made of two completely separate layers, hence model M_{111} with $K_t = K_n = 0$ is used. The relative mid-segment length is defined by $\beta = L_2/L$. The outer segments' layers are connected according to the model M_{101}. The connection between the segments is defined by the following continuity conditions: $\eta^i_{e_1}(L_1) = \eta^i_{e_2}(0)$ and $\eta^i_{e_2}(L_2) = \eta^i_{e_3}(0)$, where $\eta^i_j = u^i_j, w^i_j, \varphi^i_j, \mathcal{N}^i_j, \mathcal{M}^i_j$, where $i = a, b$, and $j = e_1, e_2, e_3$. The conditions for transverse equilibrium at the connection of the segments are $\mathcal{Q}_{e_1}(L_1) = \mathcal{Q}^a_{e_2}(0) + \mathcal{Q}^b_{e_2}(0)$ and $\mathcal{Q}^a_{e_2}(L_2) + \mathcal{Q}^b_{e_2}(L_2) = \mathcal{Q}_{e_3}(0)$. The influence of the interlayer slip modulus K_t between the layers with the segment lengths L_1 and L_3, and separation length L_2, on the beam displacements and equilibrium forces has been examined next. It is noticed that although the slip modulus has an influence on all displacements, the interlayer uplift (Δw) and distortion ($\Delta\varphi$), remain unchanged for a given value of β under a variation of K_t (Fig. 7(a)).

The interlayer uplift occurs only at the central segment where other than the applied loading, w^i depends on φ^i at the contact with the outer segments, since the segments on a single layer are

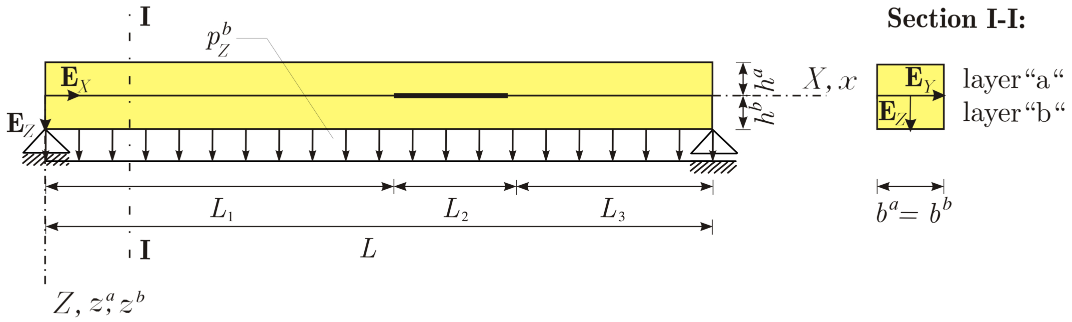

Fig. 6 Simply supported two-layer beam

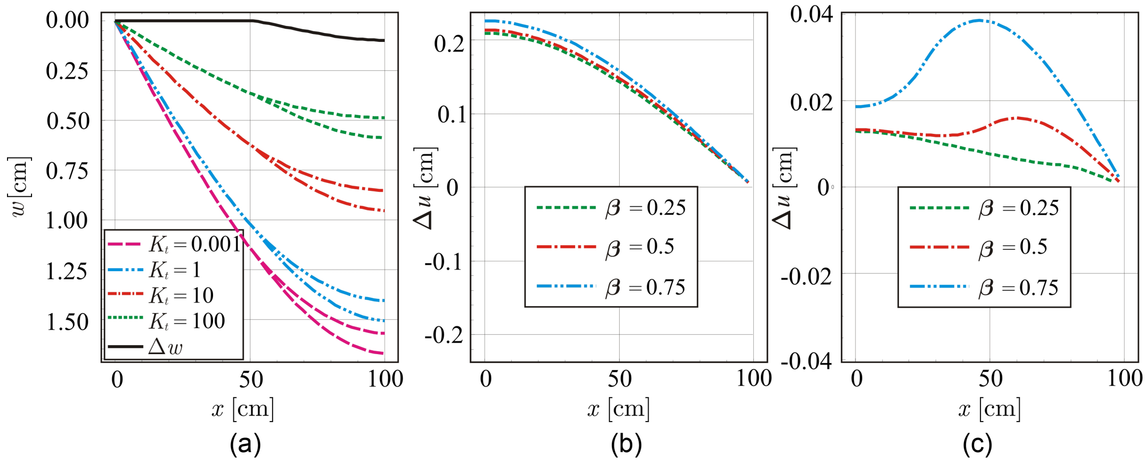

Fig. 7 (a) Vertical displacements for β = 0.5 and various K_ts, (b) Interlayer slip for K_t = 1 kN/cm^2 and various βs, (c) Interlayer slip for K_t = 100 kN/cm^2 and various βs

rigidly connected. By expanding the expression for the interlayer distortion as $\Delta\varphi = \varphi^b - \varphi^a = \gamma^b - w^{b\prime} - (\gamma^a - w^{a\prime}) = Q^b/C_2^b - Q^a/C_2^a - \Delta w'$, no dependence between $\Delta\varphi$ and K_t is noticed, since shear forces are independent of K_t (see Eq. (22)). This means that Δw is independent of K_t and so is $\Delta\varphi$ (on the entire length of the beam). Vertical displacement along the span has been plotted for $\beta = 0.5$ and different values of K_t in Fig. 7(a). The interlayer slip, Δu for $\beta = 0.25$, 0.5, 0.75, and K_t = 1,100 kN/cm^2 has been shown in Figs. 7(b) and (c). As expected, Δu, increases with decreasing of K_t and increasing the separation length.

The slip modulus K_t affects the distribution of the axial equilibrium forces and the tangential contact tractions p_t, which can be observed again for $\beta = 0.25$, 0.5, 0.75, and K_t = 1,100 kN/cm^2 in Figs. 8-9.

In case of K_t =1 kN/cm^2, the layers behave almost independently (not much difference between the inner and the outer segments) and the variation of β has little effect. In the latter case the slip modulus is high and the influence of β is more pronounced. The shear forces are, as stated earlier, independent of K_t, and so are the normal interlayer tractions (see Eqs. (11) and (9)). Their distributions are for different values of β shown in Fig. 10.

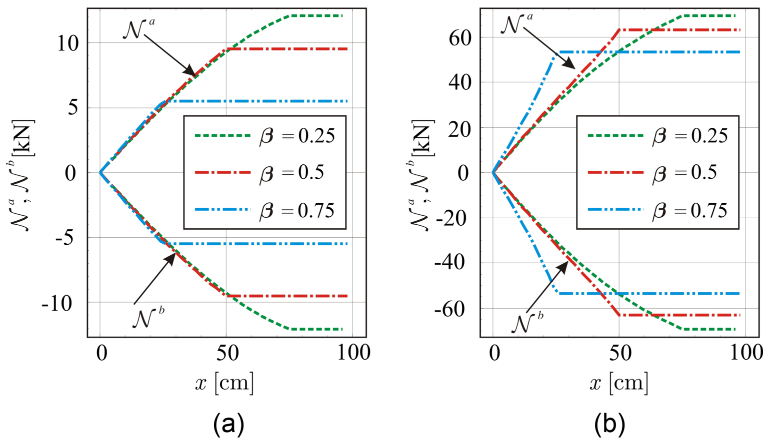

Fig. 8 Axial equilibrium forces (a) K_t = 1 kN/cm^2, (b) K_t = 100 kN/cm^2

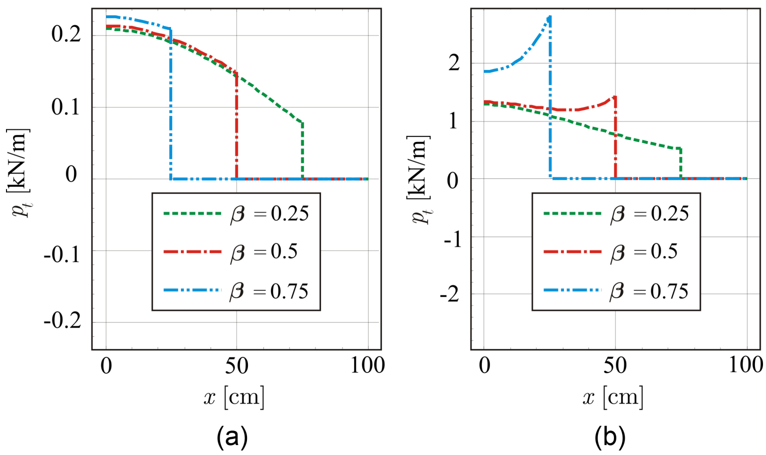

Fig. 9 Tangential contact tractions (a) K_t = 1 kN/cm^2, (b) K_t = 100 kN/cm^2

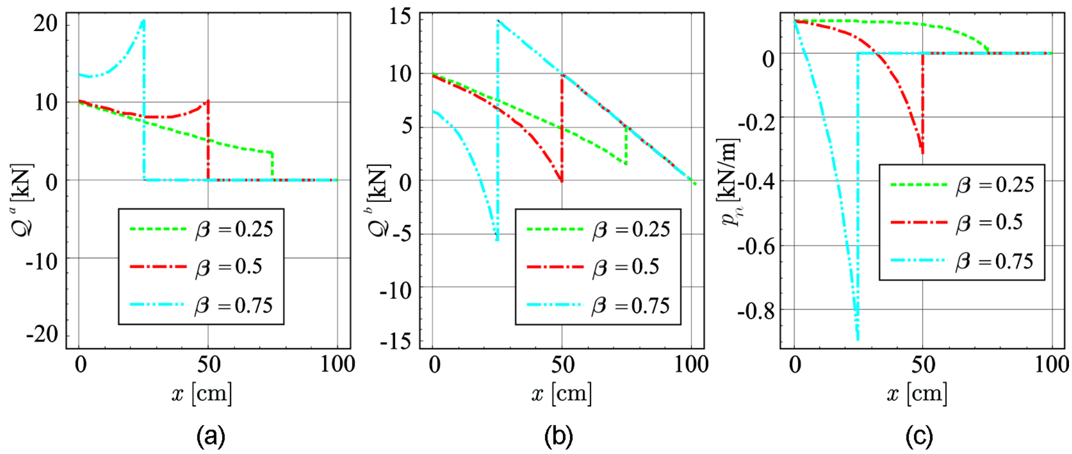

Fig. 10 Shear forces (a) layer a, (b) layer b, and (c) normal contact tractions. All quantities are K_t independent

4.3 Comments on the boundary layer effect

In the context of composite beams with interlayer slip, the boundary layer effect appears in the case of bending due to boundary moments M_0 and becomes increasingly pronounced with growing shear stiffness of the interlayer connection. When each individual layer of a two-layer beam is subjected to an end moment ($\mathcal{M}^a(0)+\mathcal{M}^b(0) = M_0$ and $\mathcal{M}^a(L)+\mathcal{M}^b(L) = M_0$) with zero axial load ($\mathcal{N}^a(0)+\mathcal{N}^b(0) = 0$ and $\mathcal{N}^a(L)+\mathcal{N}^b(L) = 0$), the normal forces in each layer and the tangential tractions at the interlayer connection emerge between the beam boundaries even though at the boundaries they do not exist.

This problem was investigated by Challamel and Girhammar (2011) for a two-layer beam with interlayer slip using the Euler-Bernoulli beam theory. In the present work the same problem is investigated using the Timoshenko beam theory. Substituting $\mathcal{M}^a = C_3^a\varphi^{a\prime}$ band $\mathcal{M}^b = C_3^b\varphi^{b\prime}$ from (20) into overall equilibrium along the beam $M_0 = \mathcal{M}^a+\mathcal{M}^b-\mathcal{N}^a\dfrac{h^a+h^b}{2}$ yields

$$M_0 = C_3^a\varphi^{a\prime}+C_3^b\varphi^{b\prime}-\mathcal{N}^a\frac{h^a+h^b}{2} \tag{29}$$

while substituting $u^{a\prime} = \mathcal{N}^a/C_1^a$ and $u^{b\prime} = \mathcal{N}^b/C_1^b$ from (20) into the derivative of (8) and the result into the derivative of $(19)_3$ and then into the derivative of $\mathcal{N}^{a\prime}+p_{t,a} = 0$ from (20) yields

$$\mathcal{N}^{a\prime\prime} = K_t\left[\mathcal{N}^a\left(\frac{1}{C_1^a}+\frac{1}{C_1^b}\right)+\frac{h^a}{2}\varphi^{a\prime}+\frac{h^b}{2}\varphi^{b\prime}\right] \tag{30}$$

Likewise, substituting $\gamma^a = \dfrac{C_3^a\varphi^{a\prime\prime}-\mathcal{N}^{a\prime}\dfrac{h^a}{2}}{C_2^a}$ and $\gamma^b = \dfrac{C_3^b\varphi^{b\prime\prime}-\mathcal{N}^{b\prime}\dfrac{h^b}{2}}{C_2^b}$ from (20) into $(19)_2$ yields

$$\varphi^a-\varphi^b-\frac{C_3^a\varphi^{a\prime\prime}-\mathcal{N}^{a\prime}\dfrac{h^a}{2}}{C_2^a}+\frac{C_3^b\varphi^{b\prime\prime}-\mathcal{N}^{b\prime}\dfrac{h^b}{2}}{C_2^b} = 0 \tag{31}$$

Solving (29) and (30) for $\varphi^{a\prime}$ and $\varphi^{b\prime}$ and substituting the result into the derivative of (31) we obtain the following fourth-order differential equation

$$c_1\frac{d^4\mathcal{N}^a}{dx^4}+c_2\frac{d^2\mathcal{N}^a}{dx^2}+c_3\mathcal{N}^a+c_4M_0 = 0 \tag{32}$$

where

$$c_1 = \frac{2C_3^aC_3^b}{K_t(C_3^ah^b-C_3^bh^a)}\left(\frac{1}{C_2^a}+\frac{1}{C_2^b}\right) \tag{33}$$

$$c_2 = \frac{2}{C_3^bh^a-C_3^ah^b}\left\{\frac{C_3^a+C_3^b}{K_t}+\left(\frac{1}{C_2^a}+\frac{1}{C_2^b}\right)\left[C_3^aC_3^b\left(\frac{1}{C_1^a}+\frac{1}{C_1^b}\right)+\frac{C_3^b(h^a)^2+C_3^a(h^b)^2}{4}\right]\right\} \tag{34}$$

$$c_3 = \frac{2(C_3^a + C_3^b)}{C_3^a h^b - C_3^b h^a}\left[\frac{1}{C_1^a} + \frac{1}{C_1^b} + \frac{(h^a + h^b)^2}{4(C_3^a + C_3^b)}\right] \tag{35}$$

$$c_4 = \frac{h^a + h^b}{C_3^a h^b - C_3^b h^a} \tag{36}$$

For the Euler-Bernoulli beam theory, shear moduli $G^i \to \infty$ and $C_2^i = k_y^i G^i A^i \to \infty$, $(i = a, b)$ reducing Eq. (32) to exactly the same form as given by Challamel and Girhammar (2011)

$$\frac{d^2\mathcal{N}^a}{dx^2} - \alpha_T^2 \mathcal{N}_1 = \beta_T M_0 \tag{37}$$

where

$$\alpha_T^2 = \frac{c_3}{c_2} = K_t\left[\frac{1}{C_1^a} + \frac{1}{C_1^b} + \frac{(h^a + h^b)^2}{4(C_3^a + C_3^b)}\right] \tag{38}$$

$$\beta_T = \frac{c_4}{c_2} = \frac{K_t(h^a + h^b)}{2(C_3^a + C_3^b)} \tag{39}$$

Using the model M_{101} and considering a simply supported two layer beam with identical geometrical and material properties as in the previous example without discontinuity in the interlayer connection ($L_2 = 0$, see Fig. 11), a numerical analysis is performed according to Challamel and Girhammar (2011).

Since for the case of pure bending no transverse forces appear, the results obtained using model M_{101} are exactly the same as the results proposed by Challamel and Girhammar (2011). Following the notation due to these authors, the dimensionless quantities are introduced

$$\hat{x} = \frac{x}{L}, \text{ and } n = \frac{\mathcal{N}^a}{\mathcal{N}_\infty^a} = \frac{\mathcal{N}^b}{\mathcal{N}_\infty^b} \tag{40}$$

where

$$\mathcal{N}_\infty^a = -\mathcal{N}_\infty^b = -\left(1 - \frac{C_3^a + C_3^b}{C_3^a + C_3^b + \dfrac{C_1^a C_1^b (h^a + h^b)^2}{4(C_1^a + C_1^b)}}\right)\frac{2M_0}{h^a + h^b} \tag{41}$$

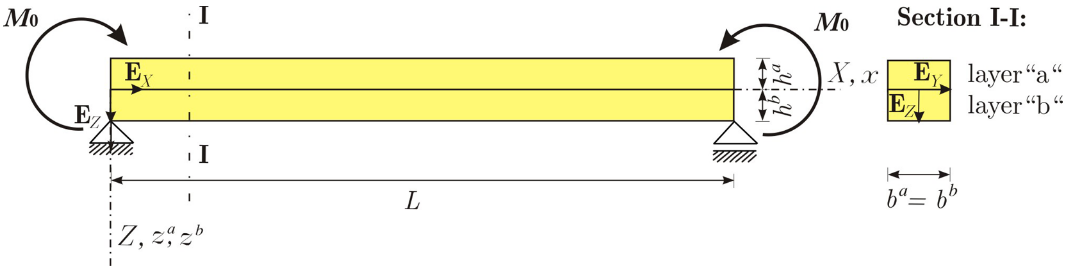

Fig. 11 Beam model for the boundary-effect analysis

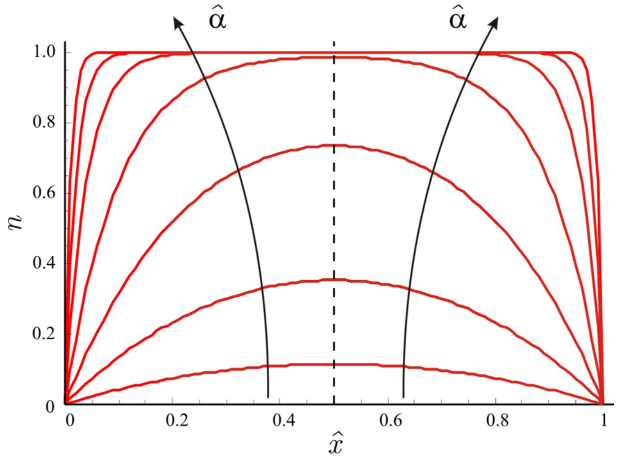

Fig. 12 Influence of the dimensionless connection parameter $\hat{\alpha}$ on the dimensionless normal force n, where $\hat{\alpha} \in \{1, 2, 4, 10, 25, 50, 100\}$

is the normal force associated with the full composite beam. In Fig. 12, the $\hat{x}-n$ diagram is shown for various values of parameter $\hat{\alpha}$, which is defined as $\hat{\alpha} = \alpha_T L$ and is proportional to the interlayer tangential stiffnesses. The results shown in Fig. 12 correspond perfectly with the results proposed by Challamel and Girhammar (2011). It is also noticed that for this example the distribution of the total moment M_0 between the layers has no influence on the normal forces, axial strains and tangential interlayer traction in the composite beam.

4. Conclusions

The paper has presented different mathematical models for analytical studying the mechanical behaviour of linear elastic multilayer Reissner's composite beam with interlayer slip and uplift between the layers. The analytical studies have been carried out to evaluate the influence of different parameters on static and kinematic quantities of multilayer beams with different combinations of contact conditions. Based on the results of this analytical study and the parametric evaluations undertaken, the following conclusions can be drawn:

1. Different interlayer contact conditions have a considerably different influence on static and kinematic quantities of multilayer beams. As a results, considerable differences in results between the models have been obtained.
2. The slip modulus has an influence on all displacements, while the interlayer uplift (Δw) and distortion ($\Delta\varphi$), remain unchanged for a given separation length under a variation of K_t.
3. The slip (Δu) increases with decreasing K_t and increasing the separation length. The shear forces are independent of K_t, and so are the normal interlayer tractions.

Acknowledgements

The results shown here have been obtained within the scientific project No 114-0000000-3025:

"Improved accuracy in non-linear beam elements with finite 3D rotations" financially supported by the Ministry of Science, Education and Sports of the Republic of Croatia and the Croatian Science Foundation project No 03.01/59: "Stability of multilayer composite columns with interlayer slip and uplift".

References

Adekola, A. (1968), "Partial interaction between elastically connected elements of a composite beam", *Int. J. Solids Struct.*, **4**(11), 1125–1135.

Alfano, G. and Crisfield, M.A. (2001), "Finite element interface models for the delamination analysis of laminated composites: mechanical and computational issues", *Int. J. Numer. Meth. Eng.*, **50**, 1701–1736.

Attard, M.M. and Hunt, G.W. (2008), "Sandwich column buckling -A hyperelastic formulation", *Int. J. Solids Struct.*, **45**(21), 5540–5555.

Bareisis, J. (2006), "Stiffness and strength of multilayer beams", *J. Compos. Mater.*, **40**(6), 515–531.

Challamel, N. and Girhammar, U.A. (2011), "Boundary-layer effect in composite beams with inter-layer slip", *J. Aerosp. Eng.*, **24**, 199–209.

Cowper, G.R. (1966), "The shear coefficient in Timoshenko's beam theory", *J. Appl. Mech.*, **33**(2), 335–340.

Frostig, Y. (2003), "Classical and high-order computational models in the analysis of modern sandwich panels", *Compos. Part B-Eng.*, **34**, 83–100.

Gara, F., Ranzi, P. and Leoni, G. (2006), "Displacement-based formulations for composite beams with longitudinal slip and vertical uplift", *Int. J. Numer. Meth. Eng.*, **65**, 1197–1220.

Girhammar, U.A. and Pan, D.H. (2007), "Exact static analysis of partially composite beams and beam-columns", *Int. J. Mech. Sci.*, **49**(2), 239–255.

Hjelmstad, K.D. (2005), *Fundamentals of Structural Mechanics*, Second Edition, Springer-Verlag, New York.

Hozjan, T., Saje, M., Srpčič, S. and Planinc, I. (2013), "Geometrically and materially non-linear analysis of planar structures with an interlayer slip", *Comput. Struct.*, **114-115**, 1-17.

Kryžanowski, A., Schnabl, S., Turk, G. and Planinc, I. (2009), "Exact slip-buckling analysis of two-layer composite columns", *Int. J. Solids Struct.*, **46**, 2929–2938.

Kroflič, A., Planinc, I., Saje, M. and Čas, B. (2010a), "Analytical solution of two-layer beam including interlayer slip and uplift", *Struct. Eng. Mech.*, **34**(6), 667–683.

Kroflič, A., Planinc, I., Saje, M., Turk, G. and Čas, B. (2010b), "Non-linear analysis of two-layer timber beams considering interlayer slip and uplift", *Eng. Struct.*, **32**, 1617–1630.

Kroflič, A., Saje, M. and Planinc, I. (2011), "Non-linear analysis of two-layer beams with interlayer slip and uplift", *Comput. Struct.*, **89**(23-24), 2414–2424.

McCutheon, W.J. (1986), "Stiffness of framing members with partial composite action", *J. Struct. Eng., ASCE*, **112**(7), 1623–1637.

Nguyen, N.T., Oehlers, D.J. and Bradford, M.A. (2001), "An analytical model for reinforced concrete beams with bolted side plates accounting for longitudinal and transverse partial interaction", *Int. J. Solids Struct.*, **38**, 6985–6996.

Perko, L. (2001), *Differential Equations and Dynamical Systems*, Third Edition, Springer-Verlag, New York.

Ranzi, G., Gara, F. and Ansourian, P. (2006), "General method of analysis for composite beams with longitudinal and transverse partial interaction", *Comput. Struct.*, **84**, 2373–2384.

Ranzi, G., Dall'Asta, A., Ragni, L. and Zona, A. (2010), "A geometric nonlinear model for composite beams with partial interaction", *Eng. Struct.*, **32**, 1384–1396.

Reissner, E. (1972), "On one-dimensional finite-strain beam theory: The plane problem", *J. Appl. Mech. Phy. (ZAMP)*, **23**, 795–804.

Schnabl, S., Planinc, I., Saje, M., Čas, B. and Turk, G. (2006), "An analytical model of layered continuous beams with partial interaction", *J. Struct. Eng. Mech.*, **22**(3), 263–278.

Schnabl, S., Saje, M., Turk, G. and Planinc, I. (2007), "Analytical solution of two-layer beam taking into account interlayer slip and shear deformation", *J. Struct. Eng. ASCE*, **133**(6), 886–894.

Schnabl, S. and Planinc, I. (2010), "The influence of boundary conditions and axial deformability on buckling behavior of two-layer composite columns with interlayer slip", *Eng. Struct.*, **32**(10), 3103-3111.

Schnabl, S. and Planinc, I. (2011), "The effect of transverse shear deformation on the buckling of two-layer composite columns with interlayer slip", *Int. J. Nonlin. Mech.*, **46**(3), 543-553.

Schnabl, S. and Planinc, I. (2013), "Exact buckling loads of two-layer composite Reissner's columns with interlayer slip and uplift", *Int. J. Solids Struct.*, **50**(1), 30-37.

Sousa, J.B.M. and da Silva, A.R. (2010), "Analytical and numerical analysis of multilayered beams with interlayer slip", *Eng. Struct.*, **32**, 1671–1680.

Timoshenko, S.P. (1940), *Strength of Materials, Part I, Elementary Theory and Problems*, 2nd Edition, D. Van Nostrand Company, New York.

Volokh, K.Y. and Needleman, A. (2002), "Buckling of sandwich beams with compliant interfaces", *Comput. Struct.*, **80**(14-15), 1329–1335.

Vu-Quoc, L., Den, H. and Ebcioğlu, K. (1996), "Multilayer beams: a geometrically exact formulation", *J. Nonlin. Sci.*, **6**, 239-270.